PROCEEDINGS OF SCIENCE

The QCD Deconfinement Critical Point for $N_f = 2$ Flavors of Staggered Fermions

Reinhold Kaiser,[a,b,*] **Owe Philipsen**[a,b] **and Alessandro Sciarra**[a,c]

[a] *Institute for Theoretical Physics - Goethe University, Max-von-Laue-Str. 1, 60438 Frankfurt am Main, Germany*

[b] *John von Neumann Institute for Computing (NIC) GSI, Planckstr. 1, 64291 Darmstadt, Germany*

[c] *Frankfurt Institute for Advanced Studies (FIAS) - Goethe University, Ruth-Moufang-Str. 1, 60438 Frankfurt am Main, Germany*

E-mail: kaiser@itp.uni-frankfurt.de, philipsen@itp.uni-frankfurt.de, sciarra@itp.uni-frankfurt.de

Quenched QCD at zero baryonic chemical potential undergoes a first-order deconfinement phase transition at a critical temperature T_c, which is related to the spontaneous breaking of the global center symmetry. Including heavy, dynamical quarks breaks the center symmetry explicitly and weakens the first-order phase transition. For decreasing quark masses the first-order phase transition turns into a smooth crossover at a Z_2-critical point. The critical quark mass corresponding to this point has been examined with $N_f = 2$ Wilson fermions for several N_τ in a recent study within our group. For comparison, we also locate the critical point with $N_f = 2$ staggered fermions on $N_\tau = 8$ lattices. For this purpose we perform Monte Carlo simulations for several quark mass values and various aspect ratios in order to extrapolate to the thermodynamic limit. The critical mass is obtained by fitting to a finite size scaling formula of the kurtosis of the Polyakov loop. Our results indicate large discretization effects, requiring simulations on lattices with $N_\tau > 8$.

The 38th International Symposium on Lattice Field Theory, LATTICE2021 26th-30th July, 2021 Zoom/Gather@Massachusetts Institute of Technology

[*] Speaker

© Copyright owned by the author(s) under the terms of the Creative Commons Attribution-NonCommercial-NoDerivatives 4.0 International License (CC BY-NC-ND 4.0).

PoS(LATTICE2021)484

1. Introduction

The nature of the thermal QCD transition at zero baryonic chemical potential has been found to be an analytic crossover for $N_{\mathrm{f}} = 2 + 1$ quark flavors with physical mass values [1]. The sign problem prohibits the exploration of the QCD phase diagram at finite baryonic chemical potentials μ_B with lattice QCD. However, investigating the nature of the thermal QCD transition at $\mu_B = 0$ for varying quark mass values with lattice QCD gives valuable insights into the phase structure of QCD. The nature of the thermal QCD transition at $\mu_B = 0$ is visualized in the Columbia plot as a function of the degenerate up- and down-quark mass value $m_{u,d}$ and the strange quark mass value m_s. First-order phase transition regions with a second-order boundary have been found with unimproved fermion discretizations on coarse lattices, for both heavy and light quark masses. In contrast to the light quark mass regime, where strong indications exist that the first order region vanishes towards the continuum limit [2], the first-order region in the heavy mass regime is known to persist from investigations of pure gauge theory [3]. A recent study with $N_{\mathrm{f}} = 2$ unimproved Wilson fermions even shows an enlargement of the first-order region when approaching the continuum limit [4].

The deconfinement transition in the heavy quark mass regime, which is subject of this work, is related to the spontaneous breaking of the Z_3 center symmetry. In the limit of infinite quark mass values, QCD is invariant under Z_3 center symmetry transformations, leading to a first-order phase transition at the transition temperature T_c. The inclusion of large but finite quark masses breaks the center symmetry explicitly. Decreasing the quark masses weakens the first-order phase transition until the deconfinement transition turns into an analytic crossover at a Z_2 second-order boundary. This Z_2-critical point has been investigated for $N_{\mathrm{f}} = 2$ quark flavors and 3 different temporal lattice extents N_τ employing the Wilson fermion action [4]. For comparison, the goal is to locate the same Z_2-critical point employing the unimproved staggered fermion action. As a first step, we present results for $N_\tau = 8$ in this work.

The motivation to study the thermal QCD transition far from the physical quark mass values is to provide a first-principles benchmark for effective theories, that are not limited by the sign problem and can access the $\mu_B \neq 0$ region. These effective theories include effective lattice theories obtained from the hopping parameter expansion [5–7] and effective Polyakov loop theories in the continuum [8, 9]. Furthermore, the Z_2-critical point is of interest, as it is the point where the latent heat of the first-order deconfinement phase transition vanishes. Hence, the dynamics of the deconfinement transition relates the value of the critical quark mass and the latent heat such that non-perturbative investigations allow valuable insights in this parameter region. For pure gauge theory with infinite quark mass values, the latent heat has already been calculated [10].

2. Simulation Details

The Monte Carlo importance sampling simulations are preformed using the standard Wilson gauge action

$$S_g = \frac{\beta}{3} \sum_n \sum_{\mu<\nu} \mathrm{Re}\left(\mathrm{Tr}\left[\mathbb{1} - P_{\mu\nu}(n)\right]\right), \tag{1}$$

PoS(LATTICE2021)484

with the inverse gauge coupling $\beta = \frac{6}{g^2}$, the plaquette $P_{\mu\nu}(n)$ depending on the lattice sites n and directions μ and ν. For the fermions, the staggered fermion action

$$S_f = \sum_n \bar{\psi}(n) \left(\sum_{\mu=1}^{4} \eta_\mu(n) \frac{U_\mu(n)\psi(n+\hat{\mu}) - U_\mu^\dagger(n-\hat{\mu})\psi(n-\hat{\mu})}{2} + (am)\psi(n) \right) \tag{2}$$

is employed, where a is the lattice spacing and $\bar{\psi}$ and ψ are the fermion fields with mass am. The gauge links are given by $U_\mu(n)$ and $\eta_\mu(n)$ is the staggered sign function. The inverse gauge coupling β controls the lattice spacing $a(\beta)$ and the temperature $T = \frac{1}{a(\beta)N_\tau}$, where $N_\tau = 8$ is the number of lattice points in temporal direction. The number of lattice points in spatial direction N_σ defines the size of the system $L = a(\beta)N_\sigma$, for which five aspect ratios $LT = N_\sigma/N_\tau \in [4, 8]$ were simulated. Simulations were run for two or three values of β around the (pseudo-)critical β_c at which the transition takes place. After a thermalization process, four independent Markov chains are produced for each β value. In order to locate the critical quark mass m_c at the Z_2-critical point, simulations were run for the mass values $am \in \{0.35, 0.55, 0.75, 0.95, 1.15\}$.

The order parameter associated with the deconfinement transition is the expectation value of the Polyakov loop L, averaged over the spatial lattice volume, with

$$L = \frac{1}{N_\sigma^3} \sum_{\boldsymbol{n}} \frac{1}{3} \mathrm{Tr} \left[\prod_{n_0=0}^{N_\tau - 1} U_0(n_0, \boldsymbol{n}) \right]. \tag{3}$$

The product is performed over all temporal gauge links at spatial lattice site $\boldsymbol{n}$, closing through the periodic boundary in temporal direction.

After 5000 trajectories of thermalization, an amount of 200k to 300k trajectories was accumulated for each Markov chain, which sums up to a maximum of 1.2M trajectories for one β value. The configurations are generated by the RHMC algorithm, where the acceptance rate is kept at $\sim 85\%$. The employed lattice QCD code is the Open-CL based code CL^{2}QCD [11], also publicly available [12], which is run on GPUs on the L-CSC cluster at GSI in Darmstadt, Germany. To manage the simulations the bash tool `BaHaMAS` was used, which allows to submit and monitor huge amounts of simulations efficiently [13].

3. Analysis of the Deconfinement Transition

We use the standardized moments skewness, B_3, and kurtosis, B_4, of the norm of the Polyakov loop to localize the deconfinement transition and determine its order. The n-th standardized moment of the expectation value of the absolute value of the Polyakov loop $|L|$ with mean value $\overline{|L|}$ is given by

$$B_n = \frac{\left\langle \left(|L| - \overline{|L|} \right)^n \right\rangle}{\left\langle \left(|L| - \overline{|L|} \right)^2 \right\rangle^{\frac{n}{2}}}. \tag{4}$$

The skewness measures the asymmetry of the distribution and serves to locate the (pseudo-)critical β_c using the condition $B_3(\beta_c) = 0$. The kurtosis of the distribution at β_c gives information about the type of the transition, which assume specific values in the infinite volume limit (see Table 1).

PoS(LATTICE2021)484

Transition type	1. Order	Z_2 (Ising 3D) [14]	Crossover
$B_4(\beta_c)$	1	1.604(1)	3

Table 1: Infinite volume kurtosis values of the order parameter for selected transitions.

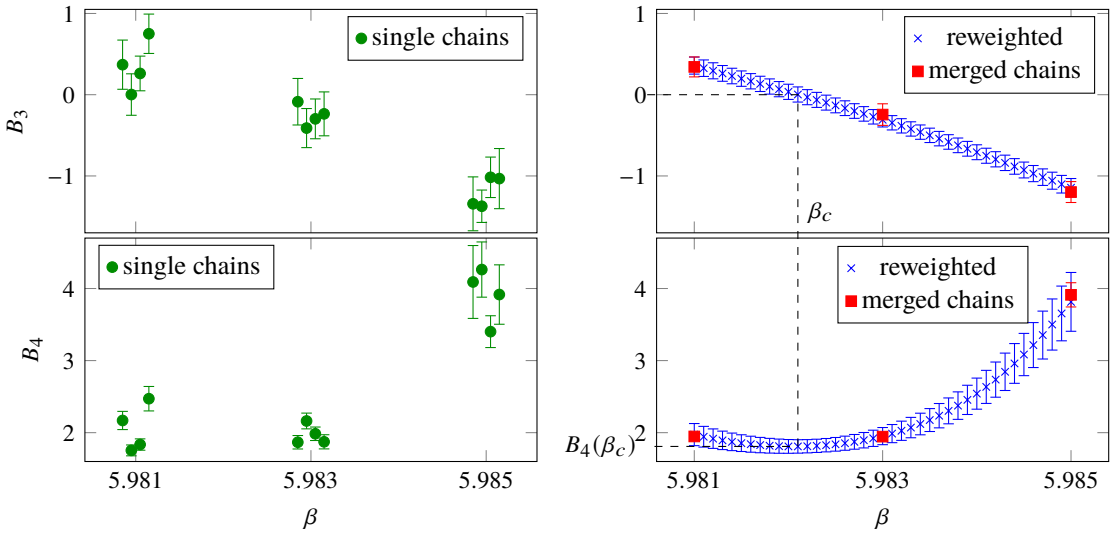

Figure 1: Exemplary analysis and reweighting of B_3 and B_4 of $|L|$ for $am = 0.55$ and $N_\sigma = 56$. The points on the left are shifted horizontally around the central value for readability. The upper row shows the skewness, the lower row shows the kurtosis. The left column shows the analysis of the independent Markov chains. The analysis of the merged chains is shown on the right in red, as well as the reweighted data points.

The sampling of the simulated β values is too coarse, such that β_c cannot be extracted directly. Interpolating the skewness and the kurtosis in between the simulated β values using the multiple histogram method [15] leads to good estimates of β_c and $B_4(\beta_c)$. This analysis strategy is visualized in Figure 1 for the parameters $am = 0.55$ and $N_\sigma = 56$.

The set of kurtosis values at β_c obtained from this analysis is volume dependent and a finite size scaling analysis has to be performed. The finite size scaling formula for the kurtosis of $|L|$, which is in general a mixture of an energy- and magnetic-like observable, is

$$B_4(N_\sigma, \beta_c, am) = \left(A + Bx + O\left(x^2\right)\right) \cdot \left(1 + C N_\sigma^{y_t - y_h} + O\left(N_\sigma^{2(y_t - y_h)}\right)\right), \tag{5}$$

with the scaling variable $x = \left(\frac{1}{am} - \frac{1}{am_c}\right) N_\sigma^{1/\nu}$ [16]. The critical exponents $y_t = 1/\nu = 1.5870(10)$ and $y_h = 2.4818(3)$ are known for the Z_2 universality class [17]. A, B, C are undetermined constants from the Taylor expansions and am_c is the value of the Z_2-critical mass in lattice units. Based on formula (5), two fit ansätze can be derived. The general one includes a correction term

$$B_4(N_\sigma, am) = \left(1.604 + b_1 \left(\frac{1}{am} - \frac{1}{am_c}\right) N_\sigma^{1/\nu}\right) \cdot \left(1 + c N_\sigma^{y_t - y_h}\right), \tag{6}$$

whereas for sufficiently large volumes N_σ the correction term can be neglected,

$$B_4(N_\sigma, am) = 1.604 + b_1 \left(\frac{1}{am} - \frac{1}{am_c}\right) N_\sigma^{1/\nu}. \tag{7}$$

PoS(LATTICE2021)484

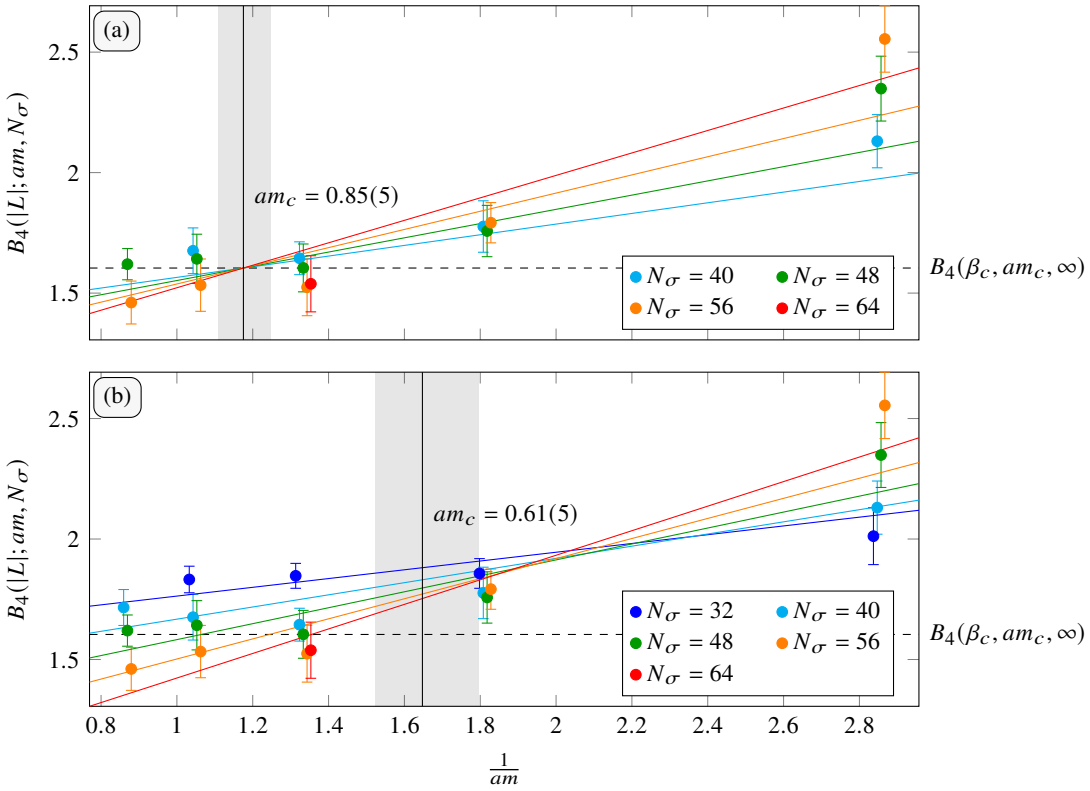

Figure 2: Kurtosis fits without and with correction term. The kurtosis points are shifted horizontally around the central value for readability. (a) shows a linear fit without correction (see formula (7)), where all points from $N_\sigma = 32$ and one point from $N_\sigma = 40$ are excluded. (b) shows a linear fit with correction (see formula (6)), where all points are included. The value of the critical quark mass is indicated by the black line and its error by the gray area.

By fitting to these fit formulas, the critical mass am_c can be extracted as a fit parameter besides the other fit parameters b_1 and c.

4. Numerical Results

Having obtained one kurtosis value at β_c for each simulated combination of N_σ and am as described in the previous section, both fit formulas (6) and (7) are fitted to this set of data. A good fit without correction is obtained by excluding the kurtosis points for the smallest volume $N_\sigma = 32$ and one point from $N_\sigma = 40$. The result is shown in Figure 2 (a). By applying the fit with correction, all simulated kurtosis points can be included and a better fit is obtained. The corresponding plot is shown in Figure 2 (b). The numerical fit results for both fits are shown in Table 2.

Comparing the plots of both fits in Figure 2, the correction term shifts the pairwise crossing point of the kurtosis lines up. This leads to a better fit, which is expressed in the better χ^2_{ndf} and fit quality parameter Q in Table 2. Especially the kurtosis points for the smallest mass value are hit much better by the fit function with correction. The results for the critical mass am_c are not compatible with each other, indicating a still large finite size effect, even if the smallest volume is

PoS(LATTICE2021)484

	m_c	b_1	c	ndf	χ^2_{ndf}	Q
fit without correction (a)	0.85(5)	0.00079(9)	-	13	1.13	32.4%
fit with correction (b)	0.61(5)	0.00063(7)	3.8(6)	17	1.03	42.1%

Table 2: Fit results for the two fits displayed in Figure 2. m_c, b_1, c are fit parameters given with their errors in parentheses. ndf is the number of degrees of freedom and χ^2_{ndf} is the χ^2 per number of degrees of freedom. The quality of the fit is quantified by the Q-parameter.

am	β_c	am_π	a {fm}	m_π {GeV}	T_c {MeV}
0.55	5.9821	1.72039(7)	0.0888(10)	3.82(4)	278(3)
0.75	6.0129	1.98121(7)	0.0872(9)	4.48(5)	283(3)

Table 3: Results from pion mass measurement and scale setting.

excluded from the fit. This statement is supported by the result of the fits with correction term, which consecutively exclude the smaller volumes. The dependence on the correction term parameter c persists, as it does not become compatible with zero when only including the largest volumes.

Regarding the considerations from above, the fit with correction term is chosen to be the best fit and the final result for the critical mass of the Z_2 critical point on $N_\tau = 8$ lattices is

$$am_c = 0.61(5). \tag{8}$$

The pion masses for the simulated quark masses are calculated at β_c on $N_\tau = 32$ and $N_s = 16$ lattices. Furthermore, the scale is set using the w_0-scale [18] based on the Wilson flow [19]. The results are shown in Table 3 for the two neighboring simulated masses around the critical mass. The pion mass in lattice units, which is larger than 1, contains significant cutoff effects, as the lattice is not able to resolve the pion represented by its Compton wavelength $1/m_\pi$.

For comparison, the results from Wilson fermions for three different $N_\tau = 6, 8, 10$ are shown in Table 4. The determination of the critical pion mass for the critical quark mass value in equation (8) for staggered fermions on $N_\tau = 8$ lattices has not yet been performed, as it is to early to use this value for a quantitative continuum extrapolation. However, the measured pion masses in Table 3 are roughly consistent with the results from Wilson fermions on $N_\tau = 8$ lattices.

N_τ	$m_\pi^{Z_2}$ {GeV}
6	5.01(5)
8	4.51(5)
10	4.39(5)

Table 4: Values of the critical pseudo scalar meson mass $m_\pi^{Z_2}$ for various N_τ from Wilson fermions [4].

5. Conclusions

This work presents a first step to determine the heavy Z_2-critical quark mass at zero chemical potential for $N_f = 2$ flavors with staggered fermions. The analysis of the fits with and without the correction term has shown a significant dependence on the correction term for obtaining good fits. To avoid the use of the correction term, simulations on much larger spatial lattices would be needed. Currently, this is not feasible as the computing time per trajectory would grow as well as the autocorrelation time of the observables due to the critical slowing down. The fact that only one

PoS(LATTICE2021)484

N_τ has been fully simulated up to this point does not allow any conclusions about the expected shift of the critical quark mass towards smaller values for increasing N_τ. The large values of the pion masses in lattice units also imply large discretization effects and the necessity to simulate on finer lattices.

Acknowledgments

The authors acknowledge support by the Deutsche Forschungsgemeinschaft (DFG, German Research Foundation) through the CRC-TR 211 "Strong-interaction matter under extreme conditions" – project number 315477589 – TRR 211 and by the State of Hesse within the Research Cluster ELEMENTS (Project ID 500/10.006). We thank the Helmholtz Graduate School for Hadron and Ion Research (HGS-HIRe) for its support as well as the staff of L-CSC at GSI Helmholtzzentrum für Schwerionenforschung for computer time and support.

References

[1] Y. Aoki, G. Endrődi, Z. Fodor, S.D. Katz and K.K. Szabó, *The order of the quantum chromodynamics transition predicted by the standard model of particle physics*, *Nature* **443** (2006) 675–678.

[2] F. Cuteri, O. Philipsen and A. Sciarra, *On the order of the QCD chiral phase transition for different numbers of quark flavours*, 2021.

[3] G. Boyd, J. Engels, F. Karsch, E. Laermann, C. Legeland, M. Lütgemeier et al., *Thermodynamics of SU(3) lattice gauge theory*, *Nuclear Physics B* **469** (1996) 419–444.

[4] F. Cuteri, O. Philipsen, A. Schön and A. Sciarra, *Deconfinement critical point of lattice QCD with $N_\mathrm{f} = 2$ Wilson fermions*, *Phys. Rev. D* **103** (2021) 014513.

[5] M. Fromm, J. Langelage, S. Lottini and O. Philipsen, *The QCD deconfinement transition for heavy quarks and all baryon chemical potentials*, *Journal of High Energy Physics* **2012** (2012) .

[6] H. Saito, S. Ejiri, S. Aoki, K. Kanaya, Y. Nakagawa, H. Ohno et al., *Histograms in heavy-quark QCD at finite temperature and density*, *Physical Review D* **89** (2014) .

[7] G. Aarts, F. Attanasio, B. Jäger and D. Sexty, *The QCD phase diagram in the limit of heavy quarks using complex Langevin dynamics*, *Journal of High Energy Physics* **2016** (2016) .

[8] C.S. Fischer, J. Luecker and J.M. Pawlowski, *Phase structure of QCD for heavy quarks*, *Physical Review D* **91** (2015) .

[9] P.M. Lo, B. Friman and K. Redlich, *Polyakov loop fluctuations and deconfinement in the limit of heavy quarks*, *Physical Review D* **90** (2014) .

[10] M. Shirogane, S. Ejiri, R. Iwami, K. Kanaya and M. Kitazawa, *Latent heat at the first order phase transition point of SU(3) gauge theory*, *Physical Review D* **94** (2016) .

PoS(LATTICE2021)484

[11] M. Bach, V. Lindenstruth, O. Philipsen and C. Pinke, *Lattice QCD based on OpenCL*, *Computer Physics Communications* **184** (2013) 2042–2052.

[12] C. Pinke, M. Bach, A. Sciarra, F. Cuteri, L. Zeidlewicz, C. Schäfer et al., *CL2QCD*, Sept., 2018. 10.5281/zenodo.5121895.

[13] A. Sciarra, *BaHaMAS*, Feb., 2021. 10.5281/zenodo.4577425.

[14] H.W.J. Blote, E. Luijten and J.R. Heringa, *Ising universality in three dimensions: a Monte Carlo study*, *Journal of Physics A: Mathematical and General* **28** (1995) 6289–6313.

[15] A.M. Ferrenberg and R.H. Swendsen, *Optimized Monte Carlo data analysis*, *Phys. Rev. Lett.* **63** (1989) 1195–1198.

[16] S. Takeda, X.-Y. Jin, Y. Kuramashi, Y. Nakamura and A. Ukawa, *Update on Nf=3 finite temperature QCD phase structure with Wilson-Clover fermion action*, *PoS* **LATTICE2016** (2017) 384 [1612.05371].

[17] A. Pelissetto and E. Vicari, *Critical phenomena and renormalization-group theory*, *Physics Reports* **368** (2002) 549–727.

[18] S. Borsányi, S. Dürr, Z. Fodor, C. Hoelbling, S.D. Katz, S. Krieg et al., *High-precision scale setting in lattice QCD*, *Journal of High Energy Physics* **2012** (2012) .

[19] M. Lüscher, *Properties and uses of the Wilson flow in lattice QCD*, *Journal of High Energy Physics* **2010** (2010) .

PoS(LATTICE2021)484